From Sliding-Rolling Loci to Instantaneous Kinematics: An Adjoint Approach

Lei Cui and Jian Dai

Dr Lei Cui

Department of Mechanical Engineering, Curtin University, Kent Road, Bentley, WA 6102, Australia

Email: lei.cui@curtin.edu.au

Tel: +61 8 9266 7594

Professor Jian S. Dai

Centre for Robotics Research, King's College London, Strand, London WC2R 2LS, United Kingdom

Email: jian.dai@kcl.ac.uk

Tel: +44 020 7848 2321

Abstract

The adjoint approach has proven effective in studying the properties and distribution of coupler curves of crank-rocker linkages and the geometry of a rigid object in spatial motion. This paper extends the adjoint approach to a general surface and investigates kinematics of relative motion of two rigid objects that maintain sliding-rolling contact. We established the adjoint curve to a surface and obtained the fixed-point condition, which yielded the geometric kinematics of an arbitrary point on the moving surface. After time was taken into consideration, the velocity of the arbitrary point was obtained by two different ways. The arbitrariness of the point results in a set of overconstrained equations that give the translational and angular velocities of the moving surface. This novel kinematic formulation is expressed in terms of vectors and the geometry of the contact loci. This classical approach reveals the intrinsic kinematic properties of the moving object. We then revisited the classical example of a unit disc rolling-sliding on a plane. A second example of two general surfaces maintaining rolling-sliding contact was further added to illustrate the proposed approach.

Keywords: adjoint, contact, rolling, sliding, kinematics, differential geometry

1 Introduction

In classical differential geometry, the adjoint approach is used to study the properties of a curve or a surface via its companion curve or surface [1, 2]. For example, the properties of an involute and evolute of a curve are studied using the geometry of the initial curve. Another example is the Bertrand curves that have common principal normal lines [3]. The famous cycloid is the locus of points traced out by a point on a circle that rolls without sliding along a straight line, where the circle is said to be adjoint to the straight line.

The adjoint approach has been applied to mechanical engineering, for example gear mesh [4]. Wang et al [5] extended the adjoint approach to investigating the coupler-curve distribution of crank-rocker linkages. The study of the moving centrode adjoint to the fixed centrode concisely revealed the distribution law of various shapes of coupler curves. They also applied the approach to the moving axodes adjoint to the fixed axodes, revealing the intrinsic properties of a point trajectory, a line trajectory, and characteristic lines on the moving body [6-8].

The sliding-spinning-rolling motion occurs naturally in many systems such as a robotic hand manipulating an object [9-11], the interaction between wheeled vehicles and the ground [12, 13], gear and cam transmission [14-16], and biomechanics [17, 18]. Developing the kinematic relation between the relative objects facilitates the subsequent dynamics or control of the systems.

The relative motion between two rigid objects that maintain sliding-rolling contact is a five degrees-of-freedom (DOFs) sliding-spinning-rolling motion, which can be decomposed into two translational sliding DOFs, $\boldsymbol{v}_1$ and $\boldsymbol{v}_2$, at the contact point and three rotational DOFs, $\boldsymbol{\omega}_1$, $\boldsymbol{\omega}_2$, and $\boldsymbol{\omega}_3$, about the contact point, as in Fig. 1.

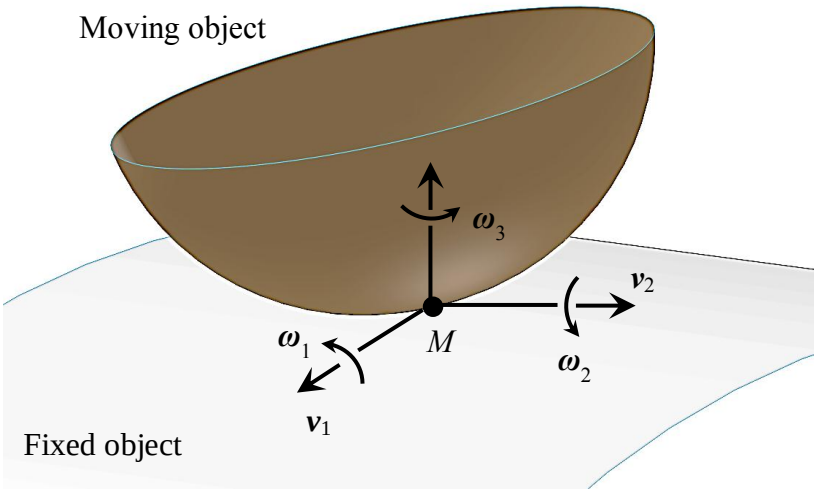

Fig. 1 The two translational sliding DOFs, $\boldsymbol{v}_1$ and $\boldsymbol{v}_2$, at the contact point and three rotational DOFs, $\boldsymbol{\omega}_1$, $\boldsymbol{\omega}_2$, and $\boldsymbol{\omega}_3$, about the contact point

Previous literature on sliding-spinning-rolling motion either restricted the shapes of objects to flat, sphere, or restricted the types of relative motion to rolling contact [19-21]. Sliding motion was sometimes singled out for dexterous manipulation [22]. For general sliding-spinning-rolling motion, the two contact points have different rates and directions, making the derivation process complicated and unintuitive. Two formulations [23, 24] have far-reaching effects on later development. The former defined one moving point trajectory and two contact trajectories to derive first- and second-order kinematics of sliding-spinning-rolling motion via Taylor series expansion. The latter derived a set of first-order kinematic equations through the velocity relation between three coordinate frames.

The results were applied to manipulations, control, and motion planning. Li, Hsu and Sastry [25] developed a computed torque-like control algorithm for the coordinated manipulation of a multifingered robot hand based on the assumption of point contact models. Sarkar, Kumar and Yun [26] extended Montana's work to include acceleration terms. By using intrinsic geometric properties for the contact surfaces, they showed the explicit

dependence on the Christoffel symbols and their time derivatives. Chen [27-31] coined the term "conjugate form of motion" for kinematics of point contact motion between two surfaces and developed a geometric form of motion representation. Han and Trinkle [32] showed all systems variables needed to be included in the differential kinematic equation used for manipulation planning and further studied the relevant theories of contact kinematics, nonholonomic motion planning. Marigo and Bicchi [33] derived analogous equations with Montana's contact equations, but with a different approach that allowed an analysis of admissibility of rolling contact.

It is natural to apply the adjoint approach to study the kinematics of the moving object, since one contact trajectory curve exists on each of the two objects. While the curve on the moving object is produced solely by rolling motion, the one on the fixed object is generated by both sliding and rolling motion. In addition, sliding motion and rolling motion are independent. Hence, there is in general an angle between these two curves.

This paper extends the adjoint approach to a curve adjoint to a general surface by adopting a purely geometric approach based on the moving-frame method [34-36]. The velocity of an arbitrary point is derived in two different ways, which yield a set of eight equations with five variables. Solving this system of overconstrained equations gives the two linear velocities and the three angular velocities.

The paper is organized as follows. Section 2 extends the adjoint approach to a general surface. Section 3 derives geometric kinematics of the moving surface in terms of contravariant vectors and geometric invariants. Section 4 derives the velocities of arbitrary point in two different ways and the arbitrariness of the point leads to the translational and angular velocities of the moving surface. Section 5 revisits the classical example of a unit disc rolling-sliding on a plane. Section 6 applies the proposed approach to general surfaces. Section 7 concludes the paper.

2 The Adjoint Approach to a General Surface

The approach of a curve adjoint to a curve and to a ruled surface has been applied to the research of the properties of coupler curves for a crank-rocker linkage [5] and the instantaneous kinematic geometry of spatial motions [6-8].

This paper extends the adjoint approach to a general surface S. A point M traces a curve Γ_M on the surface S and a frame (M-$\boldsymbol{e}_1\boldsymbol{e}_2\boldsymbol{e}_3$) moves with the point M, where the vector $\boldsymbol{e}_1$ is tangent to the curve, $\boldsymbol{e}_3$ is the normal vector of the surface S at the point M, and $\boldsymbol{e}_1$, $\boldsymbol{e}_2$, $\boldsymbol{e}_3$ are row vectors and form a right-handed orthonormal frame, as in Fig. 2.

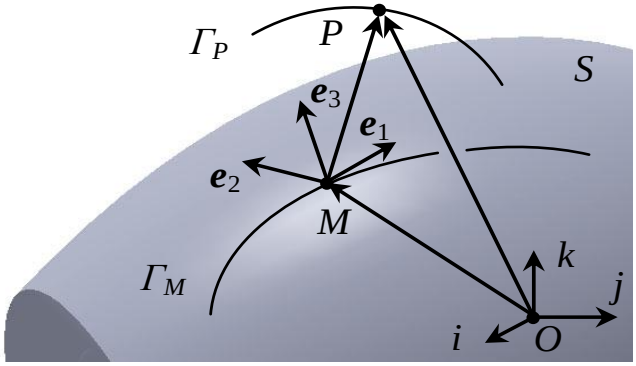

Fig. 2 The curve Γ_P adjoint to the curve Γ_M on the surface S

The moving-frame equations [34, 35] give the variations of the attached frame following the point M

$$\begin{cases} d\boldsymbol{r}_{OM}/ds = \boldsymbol{e}_1 \\ \dfrac{d}{ds}\begin{bmatrix}\boldsymbol{e}_1\\ \boldsymbol{e}_2\\ \boldsymbol{e}_3\end{bmatrix} = \begin{bmatrix} 0 & k_g & k_n \\ -k_g & 0 & \tau_g \\ -k_n & -\tau_g & 0 \end{bmatrix}\begin{bmatrix}\boldsymbol{e}_1\\ \boldsymbol{e}_2\\ \boldsymbol{e}_3\end{bmatrix} \end{cases} \tag{1}$$

where $\boldsymbol{r}_{OM}$ represents the vector from O to M with respect to (w.r.t.) the fixed frame (O-$\boldsymbol{ijk}$), s represents the arc length of the curve Γ_M, k_g, k_n, and τ_g represent the geodesic curvature, normal curvature, and geodesic torsion of the frame (M-$\boldsymbol{e}_1\boldsymbol{e}_2\boldsymbol{e}_3$) respectively.

A point P, meanwhile, traces a curve Γ_P w.r.t. the same frame (O-$\boldsymbol{ijk}$). If each position of P corresponds to a position of M, the curve Γ_P is said to be adjoint to the curve Γ_M. Hence the vector equation of Γ_P w.r.t. the frame (O-$\boldsymbol{ijk}$) is

$$\boldsymbol{r}_{OP} = \boldsymbol{r}_{OM} + u_1\boldsymbol{e}_1 + u_2\boldsymbol{e}_2 + u_3\boldsymbol{e}_3 \tag{2}$$

where $\boldsymbol{r}_{OP}$ is the vector from O to P w.r.t. the frame (O-$\boldsymbol{ijk}$), (u_1, u_2, u_3) are the coordinates of the point P w.r.t. the frame (M-$\boldsymbol{e}_1\boldsymbol{e}_2\boldsymbol{e}_3$). The derivative of the $\boldsymbol{r}_{OP}$ w.r.t. the arc length s of the locus Γ_M can be obtained by substituting the derivatives in Eq. (1) into Eq. (2) as

$$\frac{d\boldsymbol{r}_{OP}}{ds} = A_1\boldsymbol{e}_1 + A_2\boldsymbol{e}_2 + A_3\boldsymbol{e}_2 \tag{3}$$

where

$$\begin{aligned} A_1 &= 1 + \frac{du_1}{ds} - u_2k_g - u_3k_n \\ A_2 &= \frac{du_2}{ds} + u_1k_g - u_3\tau_g \\ A_3 &= \frac{du_3}{ds} + u_1k_n + u_2\tau_g \end{aligned}$$

The above equation is defined as the adjoint equation [4].

In particular, if the point P is a fixed point w.r.t. the fixed frame (O-$\boldsymbol{ijk}$), the derivative $d\boldsymbol{r}_{OP}/ds$ equals 0. Consequently the values of A_1, A_2, and A_3 are 0. It follows that

$$\begin{cases} \dfrac{du_1}{ds} = u_2k_g + u_3k_n - 1 \\ \dfrac{du_2}{ds} = -u_1k_g + u_3\tau_g \\ \dfrac{du_3}{ds} = -u_1k_n - u_2\tau_g \end{cases} \tag{4}$$

The point P in this case is called a fixed point and Eq. (4) is defined as the fixed point condition.

3 Geometric Kinematics of Sliding-Rolling Contact

Geometric kinematics studies the time-independent kinematics and the parameter actually being made use of is irrelevant [37]. The freedom to choose parameters results in a simplified analytic description of the motion. In this section, the arc lengths of the contact loci are chosen as the parameters to study the geometrical properties of the motion.

3.1 The Moving Frames on the Contact Loci

Assume that a fixed surface S and a moving surface S' maintain sliding-rolling contact at any moment. Attach the frames (O-$\boldsymbol{ijk}$) and (O'-$\boldsymbol{i'j'k'}$) to the surface S and S' respectively. Let Γ and Γ' represent the contact loci on the surface S and the surface S' respectively, as in Fig. 3.

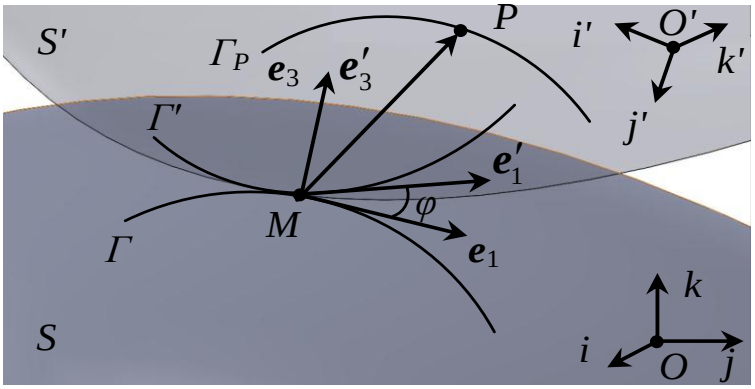

Fig. 3 The moving frames associated with the contact loci

Note that the contact locus Γ' on the moving surface S' is solely produced by rolling motion and the contact locus Γ on S is generated by both sliding and rolling motion.

Let M and M' represent the contact point on the surface S and S' respectively. These two points coincide when the two surfaces maintain point contact. We will use M to denote the contact point from now on.

Set up two right-handed orthonormal moving frames (M-$\boldsymbol{e}_1\boldsymbol{e}_2\boldsymbol{e}_3$) and ($M$- $\boldsymbol{e}_1'\boldsymbol{e}_2'\boldsymbol{e}_3'$) associated with the contact loci Γ and Γ' respectively, where $\boldsymbol{e}_1$ is the unit tangent vector of Γ, $\boldsymbol{e}_3$ is the unit normal vector of the surface S, $\boldsymbol{e}_1'$ is the unit tangent vector of Γ', $\boldsymbol{e}_3'$ is the unit normal vector of the surface S'.

Generally the direction of sliding is different from that of rolling. This gives an angle φ between the vectors $\boldsymbol{e}_1$ and $\boldsymbol{e}_1'$. The unit normal vectors $\boldsymbol{e}_3$ and $\boldsymbol{e}_3'$ can always be made to coincide when the two surfaces maintain rolling-sliding contact, as in Fig. 3.

3.2 The Fixed Point of the Moving Surface

Let P represent an arbitrary point on the moving surface S', as in Fig. 3. The position vector $\boldsymbol{r}_{O'P}$ w.r.t. the frame (O'-$\boldsymbol{i}'\boldsymbol{j}'\boldsymbol{k}'$) can be written as

$$\boldsymbol{r}_{O'P} = \boldsymbol{r}_{O'M} + u_1'\boldsymbol{e}_1' + u_2'\boldsymbol{e}_2' + u_3'\boldsymbol{e}_3' \tag{5}$$

where $\left(u_1', u_2', u_3'\right)$ are the coordinates of the point P w.r.t. the frame (M-$\boldsymbol{e}_1'\boldsymbol{e}_2'\boldsymbol{e}_3'$). Since the point P is fixed w.r.t. the frame frame (O'-$\boldsymbol{i}'\boldsymbol{j}'\boldsymbol{k}'$), the fixed point condition in Eq. (4) gives

$$\begin{cases} \dfrac{du_1'}{ds'} = u_2'k_g' + u_3'k_n' - 1 \\ \dfrac{du_2'}{ds'} = -u_1'k_g' + u_3'\tau_g' \\ \dfrac{du_3'}{ds'} = -u_1'k_n' - u_2'\tau_g' \end{cases} \tag{6}$$

where s' is the arc length of the locus Γ'. The physical meaning of s' is the distance of the contact point M travels due to rolling motion. The scalars k_g', k_n', τ_g' are the geodesic curvature, normal curvature, and geodesic torsion of the frame (M-$\boldsymbol{e}_1'\boldsymbol{e}_2'\boldsymbol{e}_3'$) respectively.

3.3 The Adjoint Curve to the Fixed Surface

The point P generates a curve Γ_P when the moving surface S' maintain rolling-sliding contact with the fixed surface S, as in Fig. 3. Hence the curve Γ_P is adjoint to the contact locus Γ. The adjoint equation (3) gives the geometric velocity of the curve Γ_P as

$$\frac{d\boldsymbol{r}_{OP}}{ds} = A_1\boldsymbol{e}_1 + A_2\boldsymbol{e}_2 + A_3\boldsymbol{e}_2 \tag{7}$$

where

$$A_1 = 1 + \frac{du_1}{ds} - u_2 k_g - u_3 k_n$$

$$A_2 = \frac{du_2}{ds} + u_1 k_g - u_3 \tau_g$$

$$A_3 = \frac{du_3}{ds} + u_1 k_n + u_2 \tau_g$$

and s is the arc length of the contact locus Γ. The physical meaning of s is the distance of the the contact point M travels due to sliding-rolling motion. The scalars (u_1, u_1, u_1) are the coordinates of the point P w.r.t. the frame (M-$\boldsymbol{e}_1\boldsymbol{e}_2\boldsymbol{e}_3$) and k_g, k_n, and τ_g represent the geodesic curvature, normal curvature, and geodesic torsion of the frame (M-$\boldsymbol{e}_1\boldsymbol{e}_2\boldsymbol{e}_3$) respectively.

3.4 The Relation between $\boldsymbol{u}$ and $\boldsymbol{u}'$

The frame (M-$\boldsymbol{e}_1'\boldsymbol{e}_2'\boldsymbol{e}_3'$) can be obtained by rotating the frame (M-$\boldsymbol{e}_1\boldsymbol{e}_2\boldsymbol{e}_3$) by an angle of φ about the $\boldsymbol{e}_3$ axis, as in Fig. 4.

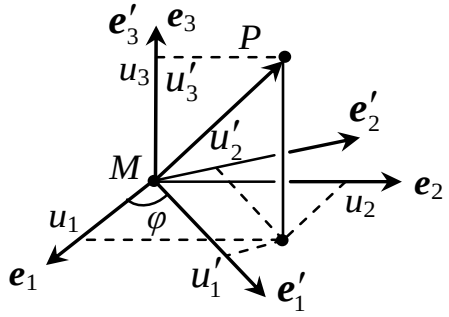

Fig.4 The coordinates of the point P in the two frames

It follows that

$$\begin{cases} \boldsymbol{e}_1' = \cos\varphi \boldsymbol{e}_1 + \sin\varphi \boldsymbol{e}_2 \\ \boldsymbol{e}_2' = -\sin\varphi \boldsymbol{e}_1 + \cos\varphi \boldsymbol{e}_2 \\ \boldsymbol{e}_3' = \boldsymbol{e}_3 \end{cases} \tag{8}$$

This leads to the coordinates (u_1, u_1, u_1) and $\left(u_1', u_2', u_3'\right)$ being related by the following equation:

$$\begin{aligned} u_1 &= u_1'\cos\varphi - u_2'\sin\varphi \\ u_2 &= u_1'\sin\varphi + u_2'\cos\varphi \\ u_3 &= u_3' \end{aligned} \tag{9}$$

Differentiating Eq. (9) w.r.t. the arc length s of the contact locus Γ yields:

$$\begin{aligned} \frac{du_1}{ds} &= \frac{ds'}{ds}\frac{d}{ds'}\left(u_1'\cos\varphi - u_2'\sin\varphi\right) = \lambda\left(\frac{du_1'}{ds'}\cos\varphi - u_1'\sin\varphi\frac{d\varphi}{ds'} - \frac{du_2'}{ds'}\sin\varphi - u_2'\cos\varphi\frac{d\varphi}{ds'}\right) \\ \frac{du_2}{ds} &= \frac{ds'}{ds}\frac{d}{ds'}\left(u_1'\sin\varphi + u_2'\cos\varphi\right) = \lambda\left(\frac{du_1'}{ds'}\sin\varphi + u_1'\cos\varphi\frac{d\varphi}{ds'} + \frac{du_2'}{ds'}\cos\varphi - u_2'\sin\varphi\frac{d\varphi}{ds'}\right) \\ \frac{du_3}{ds} &= \frac{ds'}{ds}\frac{du_3'}{ds'} = \lambda\frac{du_3'}{ds'} \end{aligned} \tag{10}$$

where λ represents the ratio of rolling rate ds' to sliding-rolling rate ds. Substituting the fix point condition du_i'/ds' in Eq. (6) into Eq. (10) yields

$$\begin{aligned}
\frac{du_1}{ds} &= \lambda\left(\left(k_g' - \frac{d\varphi}{ds'}\right)u_2 + \left(k_n' c\varphi - \tau_g' \sin\varphi\right)u_3 - \cos\varphi\right) \\
\frac{du_2}{ds} &= \lambda\left(\left(-k_g' + \frac{d\varphi_r}{ds'}\right)u_1 + \left(k_n' \sin\varphi + \tau_g' \cos\varphi\right)u_3 - \sin\varphi\right) \\
\frac{du_3}{ds} &= \lambda\left(\left(-k_n' \cos\varphi + \tau_g' \sin\varphi\right)u_1 - \left(k_n' \sin\varphi + \tau_g' \cos\varphi\right)u_2\right)
\end{aligned} \tag{11}$$

3.5 The Geometric Velocity of the Point *P*

Substituting Eq. (11) into Eq. (7) yields the geometric velocity of the point *P* as

$$\frac{d\boldsymbol{r}_{OP}}{ds} = A_1\boldsymbol{e}_1 + A_2\boldsymbol{e}_2 + A_3\boldsymbol{e}_3 \tag{12}$$

where

$$\begin{aligned}
A_1 &= 1 - \lambda\cos\varphi + \left(\lambda\left(k_g' - \frac{d\varphi}{ds'}\right) - k_g\right)u_2 + \left(\lambda\left(k_n'\cos\varphi - \tau_g'\sin\varphi\right) - k_n\right)u_3 \\
A_2 &= -\lambda\sin\varphi + \left(\lambda\left(-k_g' + \frac{d\varphi}{ds'}\right) + k_g\right)u_1 + \left(\lambda\left(k_n'\sin\varphi + \tau_g'\cos\varphi\right) - \tau_g\right)u_3 \\
A_3 &= \left(\lambda\left(-k'\cos\varphi_n + \tau_g' g\sin\varphi\right) + k_n\right)u_1 + \left(\lambda\left(-k_n'\sin\varphi - \tau_g'\cos\varphi\right) + \tau_g\right)u_2
\end{aligned}$$

This gives the geometric velocity of an arbitrary point *P* w.r.t. the arc length of the contact locus Γ, in the frame (*O*-***ijk***).

4 The Velocity of the Moving Surface: a Velocity of Two Ways

4.1 The General Form of the Velocity of the Moving Surface

An object has six DOFs, including three translational and three rotational DOFs, in three-dimensional space. When two objects maintain rolling-sliding contact, the constraint reduces one translational DOF about the direction parallel to the normal vector at the contact

point. Hence the moving surface has five DOFs, including two translational and three rotational DOFs. These five DOFs can be expressed in the frame (M-$\boldsymbol{e}_1\boldsymbol{e}_2\boldsymbol{e}_3$) via a translational velocity $\boldsymbol{v}$ and a rotational velocity $\boldsymbol{\omega}$ (see Fig. 1) as

$$\begin{aligned} \boldsymbol{v} &= v_1\boldsymbol{e}_1 + v_2\boldsymbol{e}_2 \\ \boldsymbol{\omega} &= \omega_1\boldsymbol{e}_1 + \omega_2\boldsymbol{e}_2 + \omega_3\boldsymbol{e}_3 \end{aligned} \tag{13}$$

4.2 A Velocity of Two Ways

Now the velocity of the point P can be obtained in two ways. The geometric velocity in Eq. (12) gives one form of the velocity

$$\boldsymbol{v}_P = \frac{d\boldsymbol{r}_{OP}}{dt} = \frac{ds}{dt}\frac{d\boldsymbol{r}_{OP}}{ds} = \sigma\left(A_1\boldsymbol{e}_1 + A_2\boldsymbol{e}_2 + A_3\boldsymbol{e}_3\right) \tag{14}$$

where $\sigma = ds/dt$ represent the sliding-rolling rate and the values A_1 to A_3 are identical as those in Eq. (12).

The translational and the angular velocities of the moving surface give another form of the velocity

$$\begin{aligned} \boldsymbol{v}_{OP} &= \boldsymbol{v} + \boldsymbol{\omega}\times\boldsymbol{r}_{MP} = \boldsymbol{v} + \left(\omega_1\boldsymbol{e}_1 + \omega_2\boldsymbol{e}_2 + \omega_3\boldsymbol{e}_3\right)\times\left(u_1\boldsymbol{e}_1 + u_2\boldsymbol{e}_2 + u_3\boldsymbol{e}_3\right) \\ &= v_1\boldsymbol{e}_1 + v_2\boldsymbol{e}_2 + \left(-u_2\omega_3 + u_3\omega_2\right)\boldsymbol{e}_1 + \left(u_1\omega_3 - u_3\omega_1\right)\boldsymbol{e}_2 + \left(-u_1\omega_2 + u_2\omega_1\right)\boldsymbol{e}_3 \end{aligned} \tag{15}$$

These two forms are equal, since they represent the velocity of the same point P. Hence, three scalar equations can be obtained by equalling Eqs. (14) and (15) along each of the $\boldsymbol{e}_1$, $\boldsymbol{e}_2$ and $\boldsymbol{e}_3$ directions:

$$
\begin{aligned}
&\sigma\begin{pmatrix}1-\lambda\cos\varphi+\left(\lambda\left(k_g'-\dfrac{d\varphi}{ds'}\right)-k_g\right)u_2\\ +\left(\lambda\left(k_n'\cos\varphi-\tau_g'\sin\varphi\right)-k_n\right)u_3\end{pmatrix}=v_1+\left(-u_2\omega_3+u_3\omega_2\right)\\
&\sigma\begin{pmatrix}-\lambda\sin\varphi+\left(\lambda\left(-k_g'+\dfrac{d\varphi}{ds'}\right)+k_g\right)u_1\\ +\left(\lambda\left(k_n'\sin\varphi+\tau_g'\cos\varphi\right)-\tau_g\right)u_3\end{pmatrix}=v_2+\left(u_1\omega_3-u_3\omega_1\right)\\
&\sigma\begin{pmatrix}\left(\lambda\left(-k'\cos\varphi_n+\tau'\sin\varphi_g\right)+k_n\right)u_1\\ +\left(\lambda\left(-k_n'\sin\varphi-\tau_g'\cos\varphi\right)+\tau_g\right)u_2\end{pmatrix}=-u_1\omega_2+u_2\omega_1
\end{aligned}
\tag{16}
$$

Since the point P is an arbitrary point, its coordinates, u_1, u_2 and u_3 can take arbitrary values. Thus, the coefficients of u_1, u_2 and u_3 on both sides of Eq. (16) must be equal. It follows that the first equation gives

$$
\begin{aligned}
v_1&=\sigma\left(1-\lambda\cos\varphi\right)\\
\omega_2&=\sigma\left(\lambda\left(k_n'\cos\varphi-\tau_g'\sin\varphi\right)-k_n\right)\\
\omega_3&=\sigma\left(-\lambda\left(k_g'-\frac{d\varphi}{ds'}\right)+k_g\right)
\end{aligned}
\tag{17}
$$

The second equation gives

$$
\begin{aligned}
v_2&=-\sigma\lambda\sin\varphi\\
\omega_1&=\sigma\left(-\lambda\left(k_n'\sin\varphi+\tau_g'\cos\varphi\right)+\tau_g\right)\\
\omega_3&=\sigma\left(-\lambda\left(k_g'-\frac{d\varphi}{ds'}\right)+k_g\right)
\end{aligned}
\tag{18}
$$

The third equation gives

$$
\begin{aligned}
\omega_1&=\sigma\left(-\lambda\left(k_n'\sin\varphi+\tau_g'\cos\varphi\right)+\tau_g\right)\\
\omega_2&=\sigma\left(\lambda\left(k_n'\cos\varphi-\tau_g'\sin\varphi\right)-k_n\right)
\end{aligned}
\tag{19}
$$

It can be checked that the angular velocity ω_1 in Eq. (18) equals that in Eq. (19), ω_2 in Eq. (17) equals that in Eq. (19), ω_3 in Eq. (17) equals that in Eq.(18). This completes the derivation of the velocity of the moving surface.

4.3 The Translational and Rotational Velocities of the Moving Surface

Substituting the components of translational and rotational velocity components in Eqs. (17) to (19) into Eq. (13) gives the translational and rotational velocities of the moving surface as

$$\begin{aligned}
\boldsymbol{v} &= \left(\sigma\left(1-\lambda\cos\varphi\right)\right)\boldsymbol{e}_1 - \left(\sigma\lambda\sin\varphi\right)\boldsymbol{e}_2 \\
\boldsymbol{\omega} &= \left(\sigma\left(-\lambda\left(k_n'\sin\varphi+\tau_g'\cos\varphi\right)+\tau_g\right)\right)\boldsymbol{e}_1 + \left(\sigma\left(\lambda\left(k_n'\cos\varphi-\tau_g'\sin\varphi\right)-k_n\right)\right)\boldsymbol{e}_2 \\
&\quad + \left(\sigma\left(-\lambda\left(k_g'-\frac{d\varphi}{ds'}\right)+k_g\right)\right)\boldsymbol{e}_3
\end{aligned} \tag{20}$$

There are five terms in the above equation. The two terms of the translational velocity, which are $\left(\sigma\left(1-\lambda\cos\varphi\right)\right)\boldsymbol{e}_1 - \left(\sigma\lambda\sin\varphi\right)\boldsymbol{e}_2$, give the sliding velocity of the contact point M on the tangent plane.

The first two terms of the angular velocity $\boldsymbol{\omega}$, which are along the directions of $\boldsymbol{e}_1$ and $\boldsymbol{e}_2$ respectively, give the pure-rolling motion of the moving object. The third term of the angular velocity $\boldsymbol{\omega}$ along the direction of $\boldsymbol{e}_3$ gives the velocity of spinning motion about the normal direction at the contact point M.

The angular and translational velocities in Eq. (20) are coordinate invariant, since all the entities involved are either scalars or contravariant vectors.

5. The Classical Example Revisited

Consider the classic example of a disc S' of unit radius maintaining sliding-rolling contact with a plane S while keeping the upright orientation. The contact loci are the circle Γ' of the disk and Γ on the plane. Let φ represent the angle between the curve Γ' and Γ at the contact point M; let σ represent the magnitude of the rolling-sliding rate, i.e., the arc length of Γ, let λ represent the ratio of rolling rate to sliding-rolling rate, as in Fig. 5.

Attach the moving frames frame (M-$\boldsymbol{e}_1\boldsymbol{e}_2\boldsymbol{e}_3$) and ($M$-$\boldsymbol{e}_1'\boldsymbol{e}_2'\boldsymbol{e}_3'$) to the contact loci Γ and Γ' respectively, where $\boldsymbol{e}_1$ is the tangent vector of Γ, $\boldsymbol{e}_3$ is the upward normal vector the plane S, $\boldsymbol{e}_1'$ is the tangent vector of the circle of the disc, and $\boldsymbol{e}_3'$ is the normal of the circle, pointing to the center of the disc.

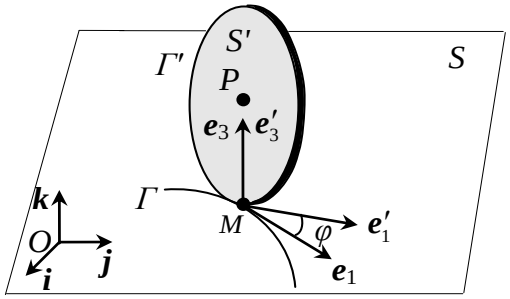

Fig. 5 A disc of unit radius sliding-rolling on a plane

5.1 The Moving-Frame Equations of the Two Loci

Let s represent the arc length of the contact locus Γ on the plane S. The moving-frame equations of the frame (M-$\boldsymbol{e}_1\boldsymbol{e}_2\boldsymbol{e}_3$) can be calculated as below.

$$\frac{d}{ds}\begin{bmatrix}\boldsymbol{e}_1\\ \boldsymbol{e}_2\\ \boldsymbol{e}_3\end{bmatrix}=\begin{bmatrix}0 & k & 0\\ -k & 0 & 0\\ 0 & 0 & 0\end{bmatrix}\begin{bmatrix}\boldsymbol{e}_1\\ \boldsymbol{e}_2\\ \boldsymbol{e}_3\end{bmatrix} \tag{21}$$

where k is the curvature of the plane locus Γ.

Let s' represent the arc length of the contact locus Γ' on the plane S'. The moving-frame equations of the frame (M-$\boldsymbol{e}_1'\boldsymbol{e}_2'\boldsymbol{e}_3'$) is

$$\frac{d}{ds'}\begin{bmatrix}\boldsymbol{e}_1'\\ \boldsymbol{e}_2'\\ \boldsymbol{e}_3'\end{bmatrix}=\begin{bmatrix}0 & 0 & 1\\ 0 & 0 & 0\\ -1 & 0 & 0\end{bmatrix}\begin{bmatrix}\boldsymbol{e}_1'\\ \boldsymbol{e}_2'\\ \boldsymbol{e}_3'\end{bmatrix} \tag{22}$$

where 1 in the matrix represent the curvature of the unit circle Γ'.

5.2 The Velocity Formulation of the Disc

Substituting the curvatures of the two contact curves in (21) and (22) into the first equation in (20) yields the translational velocity of the disc as

$$\boldsymbol{v}=\left(\sigma\left(1-\lambda\cos\varphi\right)\right)\boldsymbol{e}_1-\left(\sigma\lambda\sin\varphi\right)\boldsymbol{e}_2 \tag{23}$$

where σ is the rolling-sliding rate and λ the ratio of rolling rate ds' to sliding-rolling rate ds.

Substituting the curvatures of the two loci in Eqs (21) and (22) into the second equation in (20) gives the angular velocity of the disc as

$$\boldsymbol{\omega}=\left(-\sigma\lambda\sin\varphi\right)\boldsymbol{e}_1+\left(\sigma\lambda\cos\varphi\right)\boldsymbol{e}_2+\left(\frac{d\varphi}{dt}+\sigma k\right)\boldsymbol{e}_3 \tag{24}$$

At first sight, the above equation appears violating the geometric constraints of the disc's maintaining upright, since the angular velocity in the direction of $\boldsymbol{e}_1$ is not 0. However, the above angular velocity can be expressed in the frame (M-$\boldsymbol{e}_1'\boldsymbol{e}_2'\boldsymbol{e}_3'$) via coordinate

293 transformation by multiplying a rotation matrix:

294 $$\boldsymbol{\omega}' = (\sigma\lambda)\boldsymbol{e}_2' + \left(\frac{d\varphi}{dt} + \sigma k\right)\boldsymbol{e}_3' \tag{25}$$

295 It can be seen that the angular velocity is 0 in the direction of $\boldsymbol{e}_1'$ and thus it does not
296 violate the constraint of the disc's being upright.

297 The coordinates of the centre point P in the frame (M-$\boldsymbol{e}_1\boldsymbol{e}_2\boldsymbol{e}_3$) is (0, 0, 1). The velocity of
298 the point P can be obtained as

299 $$\boldsymbol{v}_P = \boldsymbol{v} + \boldsymbol{\omega} \times (1\boldsymbol{e}_3) = \sigma\boldsymbol{e}_1 \tag{26}$$

300 It is clear that the velocity of the circle center P is only affected by the sliding-rolling rate and
301 the direction of it is parallel to the tangent vector of the locus Γ.

302

303 **5.3 Numerical Simulation**

304 Suppose the contact locus Γ on the plane S is a circle of curvature 0.25, the rolling-
305 sliding rate σ is 1, the ratio of rolling rate to the sliding-rolling rate λ is 0.8, the angle φ
306 between rolling and sliding is a constant $\pi/6$, as in Fig. 6.

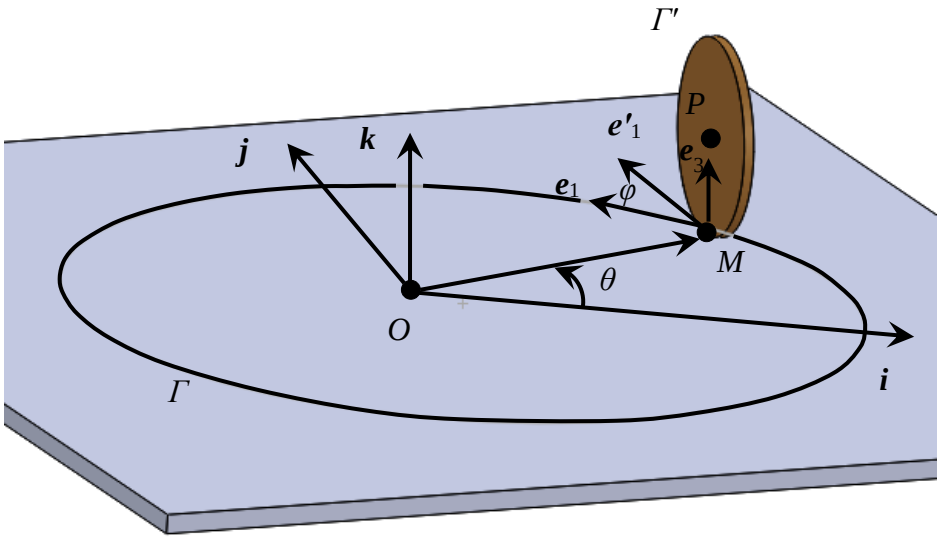

Fig. 6 A unit disk rolling-sliding along a circle of curvature 0.25

Set up a fixed frame (O-***ijk***) in such a way that the ***k***-axis is perpendicular to the plane, as in Fig. 6. Suppose the angle between the ***i***-axis and OM is θ and at the starting time $t_0 = 0$ the disc is at the intersection between the circle and the ***i***-axis. The angle θ can be obtained as $\theta = sk = t/4$, where $s = \sigma t$ is the arc length covered in the period of time t and k is the curvature of the curve Γ.

It follows that the vectors $\boldsymbol{e}_1$, $\boldsymbol{e}_2$, and $\boldsymbol{e}_3$ w.r.t. the fixed frame (O-***ijk***) are

$$\begin{aligned} \boldsymbol{e}_1 &= \left[-\sin(t/4) \quad \cos(t/4) \quad 0\right] \\ \boldsymbol{e}_2 &= \left[-\cos(t/4) \quad -\sin(t/4) \quad 0\right] \\ \boldsymbol{e}_3 &= \left[0 \quad 0 \quad 1\right] \end{aligned} \tag{27}$$

The angular velocity of the disc and the velocity of the centre point P can be obtained from Eqs. (24) and (26) w.r.t. the frame (O-***ijk***). The velocity components are plotted in Fig. 7.

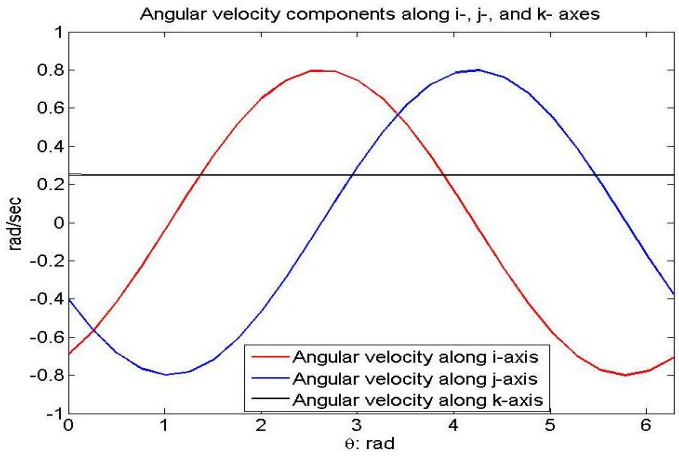

318

319 Fig. 7(a) Angular velocity components along the ***i***-, ***j***-, and ***k***-axes

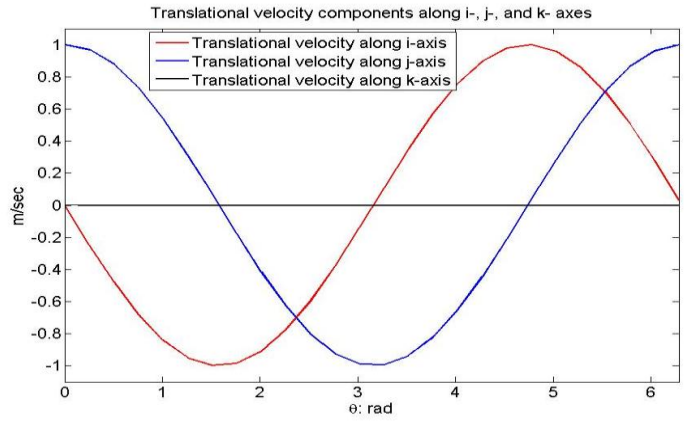

320

321 Fig. 7(b) Translational velocity components of the centre point *P* along the ***i***-, ***j***-, and ***k***-

322 axes

323

324 6 Application to Contact Trajectory Curve with Variable Curvatures

325 The proposed approach can be applied to curves and surfaces with variable geometric

326 invariants. Consider a ball of radius *r* maintaining sliding-rolling contact with a paraboloid

327 along a small circle on the sphere and a meridian on the paraboloid as in Fig. 8.

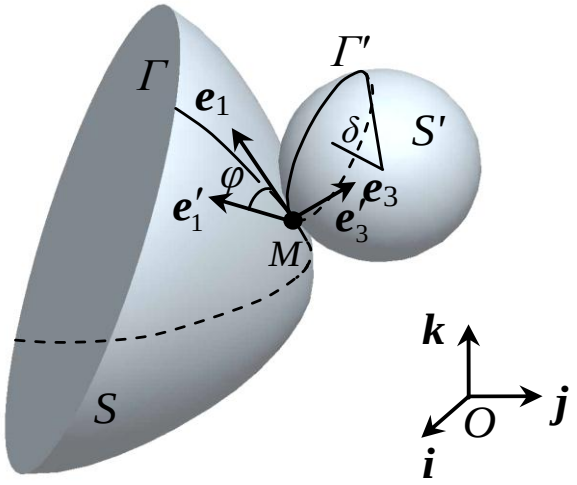

Fig. 8 A sphere sliding-rolling on a paraboloid

Suppose the paraboloid is formed by rotating a parabola $z=1/2y^2$ around z axis. A convenient reference frame can be chosen to parameterize the surfaces and contact trajectory curves. The meridian Γ can be parameterized as

$$\boldsymbol{r}\left(u,v_0\right)=\left(u,v,\frac{1}{2}\left(u^2+{v_0}^2\right)\right) \tag{28}$$

Attach the moving frames frame (M-$\boldsymbol{e}_1\boldsymbol{e}_2\boldsymbol{e}_3$) and ($M$-$\boldsymbol{e}'_1\boldsymbol{e}'_2\boldsymbol{e}'_3$) to the contact loci Γ and Γ' respectively, where $\boldsymbol{e}_1$ is the tangent vector of Γ, $\boldsymbol{e}_3$ is the outward normal vector of the surface S, $\boldsymbol{e}'_1$ is the tangent vector of the locus Γ', and $\boldsymbol{e}'_3$ is the normal of the sphere, pointing to the sphere center.

The geodesic curvature, normal curvature, and geodesic torsion of the locus Γ can be computed [38] as

$$k_g = \frac{-v_0}{\left(u^2+1\right)^{\frac{3}{2}}\sqrt{u^2+{v_0}^2+1}}$$

$$k_n = \frac{1}{\left(u^2+1\right)\sqrt{u^2+{v_0}^2+1}} \tag{29}$$

$$\tau_g = \frac{uv_0}{\left(u^2+1\right)\left(u^2+{v_0}^2+1\right)}$$

The geodesic curvature, normal curvature, and geodesic torsion of the locus Γ' can be computed as

$$k_g' = -\frac{\cot\delta}{r}, k_n' = \frac{1}{r}, \tau_g' = 0 \tag{30}$$

where δ is the half cone-angle as in Fig. 8. Substituting the curvatures of the two loci in Eqs. (29) and (30) into (20) yields the motion of the sphere as

$$\begin{aligned}
\boldsymbol{v} &= \left(\sigma - \sigma\lambda\cos\varphi\right)\boldsymbol{e}_1 - \left(\sigma\lambda\sin\varphi\right)\boldsymbol{e}_2 \\
\boldsymbol{\omega} &= \left(-\frac{\sigma\lambda}{r}s\varphi + \frac{\sigma u v_0}{\left(u^2+1\right)\left(u^2+{v_0}^2+1\right)}\right)\boldsymbol{e}_1 + \\
&\quad \left(\frac{\sigma\lambda}{r}c\varphi - \frac{\sigma}{\left(u^2+1\right)\sqrt{u^2+{v_0}^2+1}}\right)\boldsymbol{e}_2 + \\
&\quad \left(\frac{-v_0\sigma}{\left(u^2+1\right)^{\frac{3}{2}}\sqrt{u^2+{v_0}^2+1}} + \sigma\lambda\frac{\cot\delta}{r} + \frac{d\varphi}{dt}\right)\boldsymbol{e}_3
\end{aligned} \tag{31}$$

This example once again illustrates the coordinate-invariant nature of the proposed approach. It can be seen from Eq. (28) that first a convenient frame is chosen to parameterize the paraboloid and the meridian. From this local frame, the curvatures of the contact curve can be readily computed. Then the curvatures of the two contact curves are used to generate the coordinate-invariant kinematic formulation of the moving object.

7 Conclusions

This paper presented the kinematic formulation when two objects maintain sliding-rolling contact. Starting from a curve adjoint to a general surface, the paper first established the velocity of the curve and presented the fixed point conditions in terms of the arc lengths and curvatures. This adjoint approach was subsequently applied to the kinematics of two objects maintaining sliding-rolling contact. Two moving-frames were attached to the contact loci respectively, leading to the geometric velocity of an arbitrary point on the moving object. Then the velocity of this arbitrary point was derived in two various ways: one was from the previously derived geometric velocity and the other was from the translational and rotational velocity of the object. The arbitrariness of the point required these two forms of velocity to be equivalent, yielding an overconstrained system of eight equations with five variables. The angular and translational velocities were subsequently obtained by solving this overconstrained system of equations. The paper ended with two examples presented to demonstrate the proposed approach.

References

[1] A. Gray, Modern Differential Geometry of Curves and Surfaces with Mathematica, CRC Press, Inc.1996.

[2] M. Lipschutz, Schaum's Outline of Differential Geometry, Schaum's Outlines1969.

[3] P. Lucas, J.A. Ortega-Yagües, Bertrand curves in the three-dimensional sphere, Journal of Geometry and Physics, 62 (2012) 1903-1914.

[4] S. Sasaki, Differential Geometry (in Japanese), Kyolitsu Press1955.

[5] D. Wang, D.Z. Xiao, Distribution of coupler curves for crank-rocker linkages, Mechanism and Machine Theory, 28 (1993) 671-684.

[6] D. Wang, J. Liu, D.Z. Xiao, Kinematic differential geometry of a rigid body in spatial motion—I. A new adjoint approach and instantaneous properties of a point trajectory in spatial kinematics, Mechanism and Machine Theory, 32 (1997) 419-432.

[7] W. De Lun, J. Liu, X. Da Zhun, Kinematic differential geometry of a rigid body in spatial motion—II. A new adjoint approach and instantaneous properties of a line trajectory in spatial kinematics, Mechanism and Machine Theory, 32 (1997) 433-444.

[8] D.L. Wang, J. Liu, D.Z. Xiao, Kinematic differential geometry of a rigid body in spatial motion—III. Distribution of characteristic lines in the moving body in spatial motion, Mechanism and Machine Theory, 32 (1997) 445-457.

[9] L. Cui, J.S. Dai, Reciprocity-Based Singular Value Decomposition for Inverse Kinematic Analysis of the Metamorphic Multifingered Hand, ASME Journal of Mechanisms and Robotics, 4 (2012) 034502-034506.

[10] J.S. Dai, D. Wang, L. Cui, Orientation and Workspace Analysis of the Multifingered Metamorphic Hand-Metahand, IEEE Transactions on Robotics, 25 (2009) 942-947.

[11] L. Cui, U. Cupcic, J.S. Dai, Kinematic Mapping and Calibration of the Thumb Motions for Teleoperating a Humanoid Robot Hand, ASME 2011 International Design Engineering Technical Conferences and Computers and Information in Engineering Conference, ASME, Washington DC, USA, 2011, pp. 1139-1147.

[12] A. Weiss, R.G. Langlois, M.J.D. Hayes, Unified Treatment of the Kinematic Interface Between a Sphere and Omnidirectional Wheel Actuators, Journal of Mechanisms and Robotics, 3 (2011) 041001-041009.

[13] J. Agulló, S. Cardona, J. Vivancos, Dynamics of vehicles with directionally sliding wheels, Mechanism and Machine Theory, 24 (1989) 53-60.

[14] Y. Michlin, V. Myunster, Determination of power losses in gear transmissions with rolling and sliding friction incorporated, Mechanism and Machine Theory, 37 (2002) 167-174.

[15] J. Hu, M. Wang, T. Zan, The kinematics of ball-screw mechanisms via the slide–roll ratio, Mechanism and Machine Theory, 79 (2014) 158-172.

[16] S. Cardona, E.E. Zayas, L. Jordi, Radius of curvature and sliding velocity in constant-breadth cam mechanisms, Mechanism and Machine Theory, 81 (2014) 181-192.

[17] N. Sancisi, V. Parenti-Castelli, A New Kinematic Model of the Passive Motion of the Knee Inclusive of the Patella, Journal of Mechanisms and Robotics, 3 (2011) 041003-041007.

[18] R. Pàmies-Vilà, J.M. Font-Llagunes, U. Lugrís, J. Cuadrado, Parameter identification method for a three-dimensional foot–ground contact model, Mechanism and Machine Theory, 75 (2014) 107-116.

[19] L. Cui, J.S. Dai, A Darboux-Frame-Based Formulation of Spin-Rolling Motion of Rigid Objects with Point Contact, IEEE Transactions on Robotics, 26 (2010) 383-388.

[20] B. Kiss, J. Lévine, B. Lantos, On Motion Planning for Robotic Manipulation with Permanent Rolling Contacts, The International Journal of Robotic Research, 21 (2002) 443-461.

[21] K. Nomizu, Kinematics and differential geometry of submanifolds: Rolling a ball with a prescribed locus of contact, Tohoku Mathematical Journal, 30 (1978) 623-637.

[22] W. Yao, J.S. Dai, Dexterous Manipulation of Origami Cartons With Robotic Fingers Based on the Interactive Configuration Space, ASME Transactions: Journal of Mechanical Design, 130 (2008) 22303-22303.

[23] C. Cai, B. Roth, On the spatial motion of rigid bodies with point contact, IEEE Conference on Robotics and Automation, 1987, pp. 686-695.

[24] D.J. Montana, The Kinematics of Contact and Grasp, The International Journal of Robotics Research, 7 (1988) 17-32.

[25] Z. Li, P. Hsu, S. Sastry, Grasping and Coordinated Manipulation by a Multifingered Robot Hand, The International Journal of Robotics Research, 8 (1989) 33-50.

427 [26] N. Sarkar, V. Kumar, X. Yun, Velocity and acceleration equations for three-dimensional
428 contact, Journal of Applied Mechanics, 63 (1996) 974-984.
429 [27] C.-H. Chen, H.-J. Chen, d.o.f. of equivalent conjugate motion between two bodies in a
430 mechanical system, Mechanism and Machine Theory, 29 (1994) 1143-1150.
431 [28] C.-H. Chen, Conjugation form of motion representation and its conversion formulas,
432 Mechanism and Machine Theory, 32 (1997) 765-774.
433 [29] C.-H. Chen, Geometro-kinematical analysis of multi-point-conjugation joint, Mechanism
434 and Machine Theory, 32 (1997) 597-608.
435 [30] C.-H. Chen, Interdependencies between contact traces in a multi-point conjugation joint,
436 Mechanism and Machine Theory, 35 (2000) 695-716.
437 [31] C.-H. Chen, Line conjugation ruled surfaces for representation of instantaneous
438 conjugate motion of one d.o.f, Mechanism and Machine Theory, 37 (2002) 1105-1116.
439 [32] L. Han, J.C. Trinkle, The instantaneous kinematics of manipulation, IEEE International
440 Conference on Robotics and AutomationLeuven, Belgium, 1998, pp. 1944-1949.
441 [33] A. Marigo, A. Bicchi, Rolling Bodies with Regular surface: Controllability Theory and
442 Application, IEEE Transactions on Automatic Control, 45 (2000) 1586-1599.
443 [34] E. Cartan, Riemannian Geometry in an Orthogonal Frame, World Scientific Press,
444 Singapore, 2002.
445 [35] H. Cartan, Differential Forms, Dover Publisher, New York, 1996.
446 [36] L. Cui, D. Wang, J.S. Dai, Kinematic Geometry of Circular Surfaces With a Fixed
447 Radius Based on Euclidean Invariants, ASME Transactions: Journal of Mechanical Design,
448 131 (2009) 101009_101001-101008.
449 [37] O. Bottema, B. Roth, Theoretical Kinematics, Dover Publications1990.
450 [38] M.P. Carmo, Differential Geometry of Curves and Surfaces, Prentice-Hall, Englewood
451 Cliffs, 1976.